Dual Degree Project - Stage 1

Study of Solar Hydrogen System

By

Atmuri Mahesh Sreshti (18D170009)

Under the guidance of

Prof. Prakash Chandra Ghosh

Department of Energy Science and Engineering

Indian Institute of Technology Bombay

Mumbai 400076

Abstract

The importance of the integration of hydrogen production and solar energy is presented in this paper. It gives a context of the role of hydrogen and solar in the renewables sector. The science behind a solar hydrogen system is explained in detail. A thermally insulated solar hydrogen system is designed for Indian Armed Forces. Appropriate components and technologies are selected for the project. Simulink models of solar PV, electrolyser, and hydrogen storage tank have been developed. Finally, the project objectives and future goals are discussed, along with suggestions for possible future work.

Keywords: Solar hydrogen system, solar PV, electrolyser, fuel cell, hydrogen storage tank, thermally insulated system, Simulink modelling.

Table of Contents

List of Tables

List of Figures

Nomenclature

ΔG^o	Standard Gibbs Free Energy
PV	Photovoltaic
STH	Solar-To-Hydrogen
HER	Hydrogen Evolution Reaction
OER	Oxygen Evolution Reaction
PEC	Photoelectrochemical
PEM	Polymer Electrolyte Membrane / Proton Exchange Membrane
H_2O	Water
H_2	Hydrogen
O_2	Oxygen
CO_2	Carbon Dioxide
Si	Silicon
GaAs	Gallium Arsenide
CH_3OH	Methanol
K_2CO_3	Potassium Carbonate
Li_2CO_3	Lithium Carbonate
CO	Carbon Monoxide
NaOH	Sodium Hydroxide
KOH	Potassium Hydroxide
MPPT	Maximum Power Point Tracking
DC	Direct Current
PERC	Passivated Emitter and Rear Contact
P_{max}	Maximum Power
V_{mp}	Voltage at maximum power
I_{mp}	Current at maximum power
V_{oc}	Open circuit voltage
I_{sc}	Short circuit current
η	Efficiency

SOEC	Solid Oxide Electrolyser Cell
PEMFC	Polymer Electrolyte Membrane Fuel Cell
SOFC	Solid Oxide Fuel Cell
BOP	Balance Of Plant

1. Introduction

Climate change and global warming are two terms on the top of the to-solve list of every organization, industry, and government. Renewables-powered electricity generation is deemed to be one of the solutions to tackle these problems, with solar already playing a pivotal role in its implementation and success. However, solar alone cannot completely solve the renewables jigsaw. Storage is a massive hurdle in the successful implementation of these renewable as they are intermittent in nature. To tackle this, a considerable amount of research is going into batteries and other storage options. One exciting option to store solar energy is in the form of hydrogen. Hydrogen is a carrier of energy and can potentially solve the problem of clean and green fuels, provided its generation is from non-carbon sources. Hence combining solar energy with hydrogen production can lead to carbon-free fuel, at least during operation. It provides a clean alternative to fossil fuels, contributes to job creation and economic prosperity even in lesser developed areas.

A significant amount of research on hydrogen as a fuel has led to progress in applications such as rocket propulsion, IC engines, and fuel cell vehicles. Many countries have pledged and are taking steps towards a hydrogen economy, giving a much-needed boost to research and development. However, there are many problems that this technology needs to overcome before commercialization.

At high altitudes and strategic locations, it is incredibly challenging for the army to carry supplies or refill them regularly, and it also becomes a costly affair. The oxygen levels at such high altitudes are very low, and the energy supply is not very feasible. Also, the sub-zero temperatures mean that nights must be spent in extreme conditions. Hence, there is a need for electricity, fuel (hydrogen), oxygen, and heat for the armed forces. This is where the solar hydrogen technology can step in and bridge the gap between necessities and actions.

The aim of this project is to engineer a huge multifunctional thermally insulated vessel of approximate dimensions 20 ft x 6 ft x 6 ft powered by solar energy. Solar energy is used to generate electricity, which will power the load and run an electrolyser. The produced hydrogen can be utilised later as a fuel. This system is being engineered with the ambition of usage by the Indian Armed Forces. It will act as a multi-purpose vessel producing electricity for general usage and electrolysis, producing hydrogen, oxygen, and warmth in the vessel. The operation of electrolyser and fuel cell leads to heat evolution since they are not 100% efficient. This energy is lost in the form of heat, which can warm up the system and maintain temperature with thermal insulation technology.

In this report, the focus will be on the following points

- Chapter 2 explains the basics of a solar hydrogen system
- Chapter 3 describes the working of system and selection of components/materials
- Chapter 4 analyses the mathematical models of solar hydrogen subsystems
- Chapter 5 concludes the current work with inferences and insights
- Chapter 6 explores the future possibilities and the scope of this project

2. Solar Hydrogen System

Hydrogen can be produced by different methods, including natural gas reforming/gasification, electrolysis, and fermentation. Unlike other methods, electrolysis can potentially convert water to hydrogen without any carbon emissions. This is possible provided the electricity is from a renewable source or non-carbon-emitting fuel. Splitting of water into hydrogen and oxygen is an endothermic reaction, i.e., it requires energy to complete the reaction. Production of one mole of hydrogen requires 237 kJ of free energy under standard conditions. [6]

$$H_2O \rightarrow H_2 + \tfrac{1}{2} O_2 \qquad \Delta G^o = +237 \text{ kJ/mol}$$

There are multiple renewable sources which can be coupled with electrolysis to produce "green hydrogen." This study focuses on solar energy as the renewable source as it is abundant and immensely available worldwide. It is an appealing method of storing chemical energy and providing "green hydrogen" to the industry. Using such a storage system also helps solve some of the challenges associated with the intermittency of solar energy, unfavourable sunshine conditions, and seasonal storage.

Over the last few decades, intensive research led to a significant improvement in the solar-to-hydrogen (STH) efficiencies and stability of the solar water splitting devices. Nevertheless, this method did not reach the competitive levels yet with other large-scale hydrogen production technologies that produce in excess of 50 million t/yr from non-renewables worldwide. Current researchers focus on increasing the lifetime, improving efficiency/performance, and, most importantly, reducing the cost of eventual large-scale implementation. [1]

2.1 Types of Solar Hydrogen Systems

There are mainly 4 types of solar hydrogen systems: photocatalytic, photoelectrochemical, photobiological, and solar thermal.

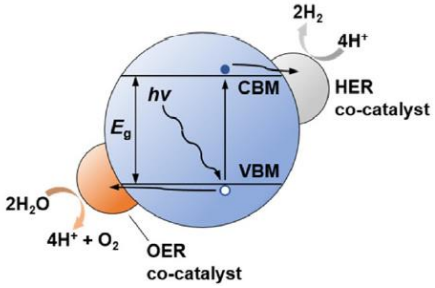

Fig 2.1 Single semiconductor: Mechanism of photocatalytic water splitting [4]

2.1.1 Photocatalytic

When a photon of energy higher than the bandgap of semiconductor is incident, an electron is excited from its valence band to the conduction band leaving behind a hole. For the

hydrogen evolution reaction (HER) and oxygen evolution reaction (OER) to begin, these electrons and holes must be separated and diffused to the semiconductor's exterior. [4]

2.1.2 Photoelectrochemical

There are three methods by which PEC devices convert solar irradiance to hydrogen: fully integrated / wireless, partially integrated / wired, non-integrated / modular. In the first type, the fully integrated / wireless devices, the solar module and the electrocatalysts are in direct touch. In the partially integrated / wired photoelectrochemical devices, one of the oxidation side or reduction side catalyst is in direct contact with the solar module, while the catalyst on the other electrode is externally connected via electrical wires. Both fully integrated and partially integrated devices convert sunlight to hydrogen via electrolysis in a single device. [1]

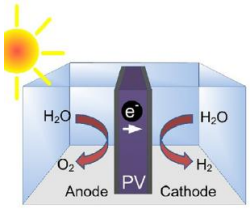

Fig 2.2 Fully integrated device [4]

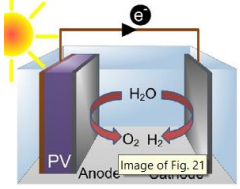

Fig 2.3 Partially integrated device [4]

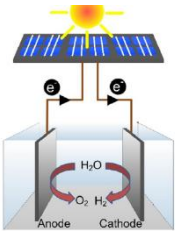

Fig 2.4 Non-integrated device [4]

The third type of devices, the non-integrated devices also called modular devices comprise of 2 discrete components: PV cells and electrolyser. These two components are connected externally via electrical wiring to produce hydrogen. [4]

2.1.3 Photobiological

Photobiological hydrogen production has received greater attention in the past two decades as an upcoming technology for industry scale H_2 production owing to its effectively negative carbon footprint and harmless biochemical reaction conditions. Microalgae, purple non-sulfur bacteria (PNSB), and cyanobacteria have shown photobiological hydrogen evolution through different mechanisms. [4]

Cyanobacteria and microalgae exhibit an activity that syncs with the irradiance-reliant levels of photosynthesis called direct biophotolysis of water. Guided by photocatalytic reactions, electrons are first removed from H_2O & then transported to redox intermediary ferredoxin. Hydrogenases extracts electrons from the reduced ferredoxin in place of embedding carbon dioxide through the irradiance-unrestrained reactions of photosynthesis. This catalyses the HER utilizing the protons extracted from water. [4]

2.1.4 Solar Thermal

Concentrated solar energy is utilised to achieve higher temperatures in a reaction chamber to steer the electrolysis process. This phenomenon is also known as solar thermal water splitting, another method towards the production of “green hydrogen.” Solar collectors and receivers of different concentration factors, dimensions, and power capacities have been developed over the years for various solar thermal applications worldwide. Some of them

include concentrating collector, flat plate collector, parabolic collector, and vacuum tube collector. Hence it is practical to integrate a thermochemical water splitting device with an existing solar thermal power plant/device matching their power capacities. [5]

2.2 Types of Photoelectrochemical (PEC) Solar Hydrogen Systems

Photoelectrochemical water splitting devices are classified into three categories depending on how the electrolysis device and light absorber are connected/integrated. They are fully integrated / wireless, partially integrated / wired, non-integrated / modular.

2.2.1 Fully Integrated/Wireless

Attempts to make a fully integrated device started in 1990s. OER and HER catalysts were sputtered into amorphous silicon solar cells (triple junction) (0.27 cm^2 active area). Perovskites were also tried as light absorbers for these devices but failed due to their vulnerability on exposure to moisture. Although the fully integrated devices are more economically viable than wired versions, they are lesser efficient. They need to be encapsulated to prevent damage of the solar cells. Also, any disturbances in the liquid electrolyte might cause optical disturbances in the form of bubbles reducing their STH efficiencies. [4]

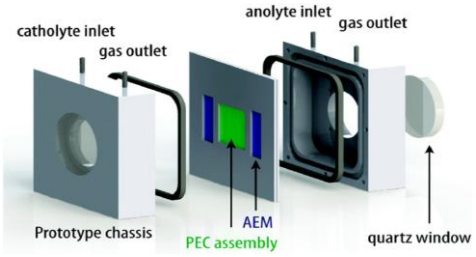

Fig 2.5 Fully integrated system [4]

2.2.2 Partially Integrated/Wired

A highly publicised partially integrated device had a p-type $GaInP_2$ photocathode coupled with a GaAs p-n junction. The solar to hydrogen efficiency of this device was reported as 12.4%. There were many more demonstrations of different silicon based solar cells as the light absorber with higher active areas but with lower STH efficiency due to the problems of scaling up the devices. Researchers came up with photoelectrodes composed of abundantly available earth materials. [4]

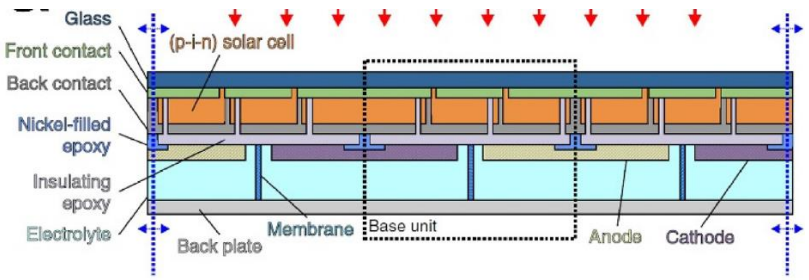

Fig 2.6 Cross-sectional view of a PV water-splitting device [4]

2.2.3 Non-Integrated/Modular

For scaling up solar hydrogen production at an industrial scale, modular devices seem to be the best bet going forward as they are very simple in comparison to other integrated devices. They are just a combination of common photovoltaic modules and electrolysers. Modular devices can be of two types: membrane-based and membraneless electrolyser-based system. Within membrane-based devices, there are alkaline electrolysers and polymer electrolyte membrane electrolysers (PEM).

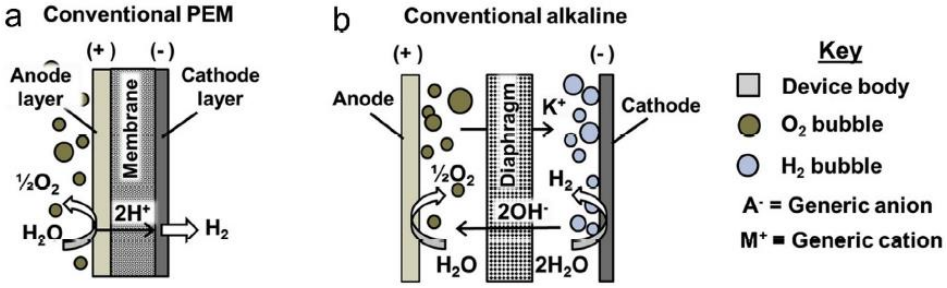

Fig 2.7 Cross-sectional view of PEM, alkaline electrolysis cells [4]

In membraneless devices, there are two types of devices: flow-by electrodes (Type I) and flow-through electrodes (Type II). In flow-by electrodes, H_2 and O_2 which are flowing along the electrode surfaces are carried by aqueous electrolyte. They are separated in the downstream area with H_2 and O_2 rich electrolytes. In flow-through electrodes, the electrolyte flows through the electrode crevice in the metallic mesh. This carries the products into respective channels. [4]

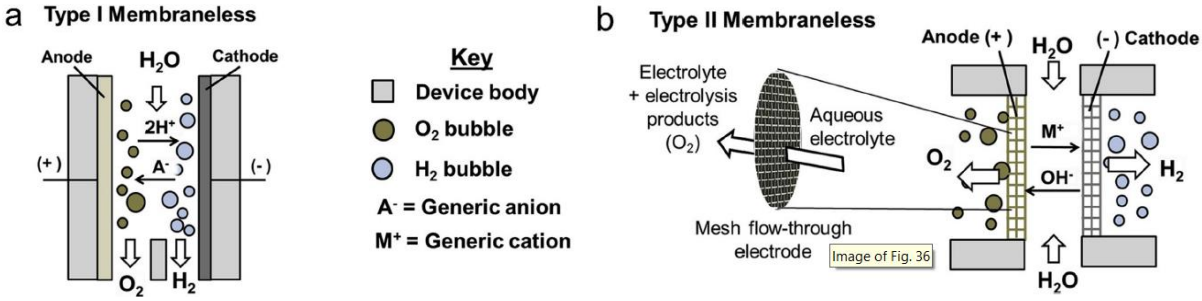

Fig 2.8 Cross-sectional view of flow-by, flow- through electrodes [4]

2.3 Solar Hydrogen Systems Examples

Ever since the world's first solar-powered hydrogen production plant became operational in 1990 in Southern Germany [7], hundreds of researchers and industries tried to develop different types of solar hydrogen systems. Multiple technologies of solar PV were tried to power the electrolyser, ranging from amorphous Si solar cells to GaAs solar cells. Electrolysers and fuel cells were mainly of alkaline or PEM technology, but a plethora of electrolytes and electrodes were tested in the alkaline versions. As the research advanced and as more people contributed towards this technology, the efficiency, life, stability, and cost have reasonable improved. Some examples of solar hydrogen systems from around the world are shown in Table 2.1. [1][4][6][8][9][10]

#	Components/Project Name	Solar Module/Cell	PV efficiency	Electrolyser	STHmax efficiency	Hydrogen Storage	Fuel Cell
[1]	PEM-EC, Solar cells	bifacial Si heterojunction	18.4% (30% albedo)	PEM	15.50%		-
		monofacial Si heterojunction	16.40%		13.70%		
[4]	-	InGaP/GaAs/GaInNAsSb triple-junction, highest STH	-	2 PEM	30%		-
		GaInP/GaAs/Ge multi-junction		10 cm2 Ni foam electrodes in 1 M NaOH	22.40%		
		a-Si:H/a- Si:H/ μc-Si:H triple junction		two Ti sheet electrodes loaded with Pt and IrO x catalysts	4.80%		
		Perovskite solar cells		bifunctional NiFe catalyst-loaded Ni foams as electrodes	12.30%		
		III–V solar cells		PEM	18%		
[6]	PV cell, photon-enhanced thermionic emission cell, SOEC	multi-junction GaAs PV cell	29.8% and 37.2% for triple-junction & quadruple-junction	Solid Oxide Electrolysis Cell	29.61%		-
[15]	FIRST (2000-2004)	1.4 kWp, monocrystalline Si		PEM, 1 kW		Metal hydrides, 30 bar, 70 Nm3 volume cap, 248 kWh	PEM, 0.42 kW
	INTA (1989-97)	8.5 kWp	10% (avg)	Alkaline, 5 kW	7.05%	Metal hydrides - pressurized tanks, 200 bar, 24-9 Nm3 volume cap, 85-32 kWh	PAFC-PEM, 10-7.5 kW
	PHEOBUS (1993-2003)	43 kWp		Alkaline, 26 kW		Pressurized tank, 120 bar, 3000 Nm3 volume cap, 10638 kWh	PEM, 5.6 kW
	SAPHYS (1994-97)	5.6 kWp, monocrystalline Si		Alkaline, 5 kW		Pressurized tank, 200 bar, 120 Nm3 volume cap, 426 kWh	PEM, 3 kW
	SCHATZ (1989-96)	9.2 kWp, monocrystalline Si		Alkaline, 6 kW	6.2% (avg)	Pressurized tank, 8 bar, 60 Nm3 volume cap, 213 kWh	PEM, 1.5 kW
	Solar house (1992-95)	4.2 kWp		PEM 2 kW		Pressurized tank, 28 bar, 400 Nm3 volume cap, 1418 kWh	PEM, 3.5 kW
	Solar hydrogen pilot plant (1990-92)	1.3 kWp	13% (avg)	Alkaline 0.8 kW	9.27% (avg)	Pressurized tank, 25 bar, 200 Nm3 volume cap, 709 kWh	PAFC, 0.5 kW
	SWB (1989-96)	370 kWp, monocrystalline, polycrystalline and amorphous Si	9-13% (crystalline) & 5% (amorphous)	Alkaline 100 kW		Pressurized tank, 30 bar, 5000 Nm3 volume cap, 17730 kWh	PAFC, 80 kW
	CEC (2007-)	5 kWp		Alkaline 3.35 kW		Metal hydrides, 14 bar, 5.4 Nm3 volume cap, 19 kWh	PEM, 2.4 kW
[16]	solar cells, electrolyser, hydrogen storage tank, fuel cell			PEM	CHP fuel cell ~ 72%		PEM, 0.5 kW
[17]	PVT modules, electrolyser, fuel cell stack, battery, H2 storage tank, H2 compressor	PVT modules	9% (overall electrical energy efficiency)	PEM	14.5% (max net energy efficiency)		PEM

Table 2.1 Examples of solar hydrogen systems

3. System Design and Selection of Components

Designing a fully functional solar hydrogen system would require an extensive design of the system. This can be done by ensuring that every subsystem is compatible with each other and contributes towards the ultimate goal of utilizing maximum possible amount of energy.

3.1 System Design for Simulation

The solar hydrogen system is being developed by the logical combination of the following components and subsystems: solar PV array, MPPT solar charge controller, DC-DC converter, electrolyser, hydrogen storage, oxygen storage, fuel cell, water storage, load, thermally insulated system, battery. The below flowchart shows the dependencies of each subsystem on others and the overall functioning of the system.

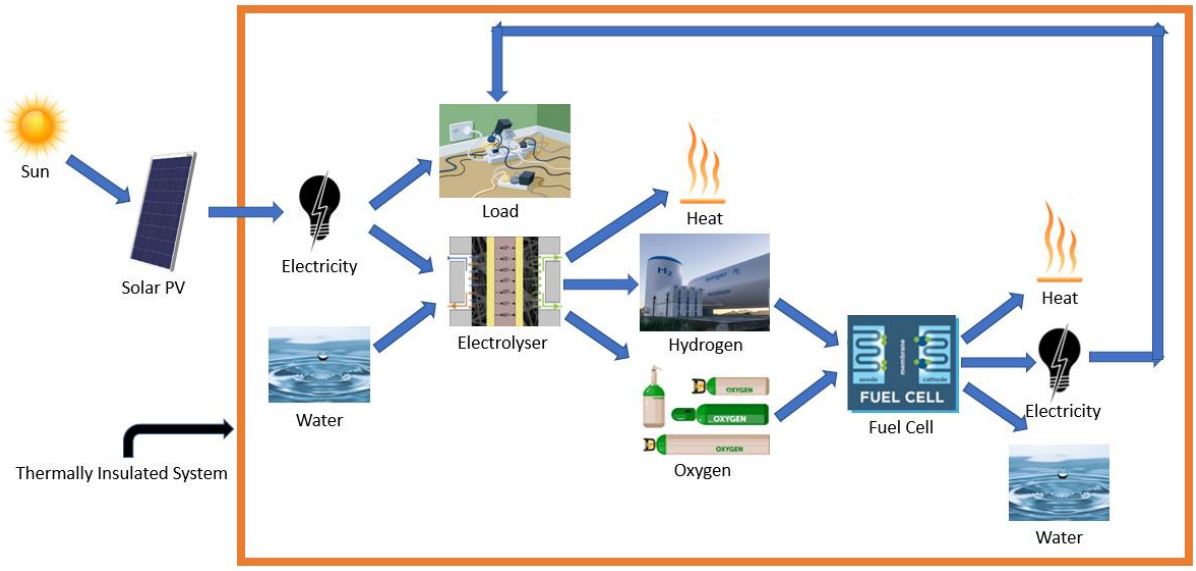

Fig. 3.1 Flowchart of thermally insulated solar hydrogen system

Energy is provided to the system by sun rays. Incident solar radiation is captured by the solar panels and converted to electricity. This electricity is used to fulfil the load demand. System is designed in such a way that the electricity produced by solar PV in active sunshine hours is more than the peak load in the same time. This ensures that there is always electricity which is unused by the load. The unused energy drives the electrolyser to produce hydrogen and oxygen, along with heat due to inefficiencies. Both the hydrogen and oxygen are stored in separate storage tanks/cylinders. When there is insufficient sunlight to meet the load demand or during non-sunshine hours, the stored hydrogen is used in fuel cell to produce electricity, water, and heat. Hydrogen can also be stored for long term usage in fuel cells in colder seasons with less or no sunlight. Depending upon the final sizing, battery may or may not be used in the system as a backup storage option or to improve the energy efficiency of the system. The thermally insulated space prevents heat loss to external environment, increasing the total energy utilization. All the heat released during the operation of electrolyser and fuel cell is captured leading to higher internal temperature of the space.

Selection of components for each subsystem is discussed in the following subsections.

3.2 Solar PV Selection

Since the first ever solar cell made in 1883, a number of solar photovoltaic technologies have come up with varying advantages, applications, and costs. For the current study, the following technologies are considered: monocrystalline Si, polycrystalline Si, monocrystalline Si PERC, thin film, perovskite. Other technologies like Gallium Arsenide and III-V solar cells have been omitted from the comparison due to their extremely high cost in comparison to major technologies in the market.

In monocrystalline Si PERC, the acronym PERC stands for Passivated Emitter & Rear Contact. Mono Si is cheaper than mono Si PERC, but PERC cells are more efficient than the conventional mono Si. Hence the cost per unit energy becomes almost equal for both the technologies. So mono Si PERC is preferred over mono Si.

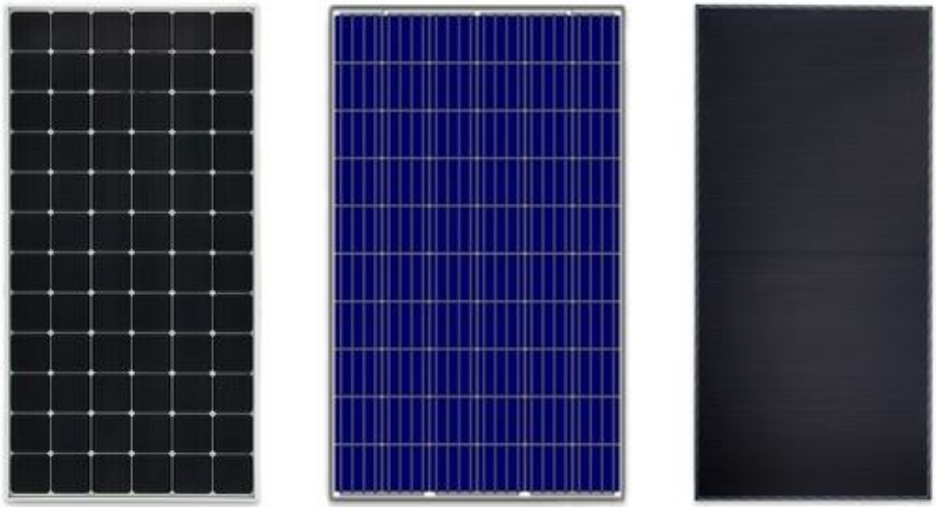

Fig. 3.2 Monocrystalline, polycrystalline, and thin film solar modules. Source: internet

Monocrystalline and polycrystalline Si solar cells are very mature technologies due to decades of research and industrial applications. Polycrystalline Si cells are cheaper than their monocrystalline counterparts, but they are also less efficient in comparison. Polycrystalline cells perform worser in higher temperatures due to their higher temperature coefficients. Both of them have a very good life of about 25 years. The following tables help in comparison of monocrystalline Si PERC and polycrystalline Si solar cells. The data has been taken from the datasheets of Vikram Solar polycrystalline and monocrystalline solar cells.

Peak Power P_{max} (W)	315	320	325	330	335	340
Max Voltage V_{mpp} (V)	37.5	37.7	37.8	38	38.1	38.2
Max Current I_{mpp} (V)	8.4	8.5	8.6	8.7	8.8	8.91
Open Circuit Voltage V_{oc} (V)	45.8	46	46.2	46.3	46.5	46.7
Short Circuit Current I_{sc} (A)	8.92	9.03	9.13	9.24	9.35	9.46
Module Efficiency (%)	16.23	16.49	16.75	17.01	17.26	17.52

Table 3.1 Vikram Solar Eldora polycrystalline Si PV modules. Source: internet

Peak Power P_{max} (W)	365	370	375	380	385
Max Voltage V_{mpp} (V)	39.8	40.0	40.1	40.2	40.3
Max Current I_{mpp} (V)	9.17	9.26	9.36	9.46	9.56
Open Circuit Voltage V_{oc} (V)	48.3	48.5	48.7	48.8	48.9
Short Circuit Current I_{sc} (A)	9.73	9.84	9.94	10.04	10.14
Module Efficiency (%)	18.81	19.07	19.33	19.58	19.84

Table 3.2 Vikram Solar Somera monocrystalline Si PERC PV modules. Source: internet

Both monocrystalline PERC and polycrystalline have same module area in the above tables. It can be concluded that monocrystalline Si PERC, although slightly expensive are much more efficient and perform better compared to polycrystalline Si solar modules.

Perovskite solar cells' efficiency has seen a steep rise in the last decade, reaching efficiencies greater than 25%. But none of these could be scaled up for commercial uses, they were lab-scale. Due to their low life and instability in ambient conditions like humidity and high cell temperature, perovskite solar cells are unsuitable for commercial applications yet.

Thin film solar cells have a very unique advantage of being foldable and look aesthetically good. Shading and high temperatures do not have a significant impact on this technology. But they are much lesser efficient compared to even polycrystalline Si solar cells. They also degrade faster than the crystalline solar cells, leading to shorter life-span.

On the basis of the above discussion, monocrystalline Si PERC solar cells have been finalized as the technology to be used for this project.

3.3 Electrolyser Selection

An electrolyser is a system that uses electricity to break water into hydrogen and oxygen. It also produces heat in the process due to the impossibility of 100% efficiency. There are mainly three types of electrolysers namely alkaline, proton exchange membrane (PEM), and solid oxide. Depending on the electrolyte material being used in them, these electrolysers vary slightly in their function.

Alkaline electrolysers use a liquid electrolyte solution like potassium hydroxide (KOH) or sodium hydroxide (NaOH), and water (H_2O). They are the oldest type of electrolysers, dating back to the early 19th century, and well established too. Thus, it is the cheapest available option for electrolysis, cheaper than both PEM and Solid Oxide electrolysers. They use non noble catalysts and have good long-term stability. But they suffer with low current densities, crossover of gases, and corrosive liquid electrolyte. [20]

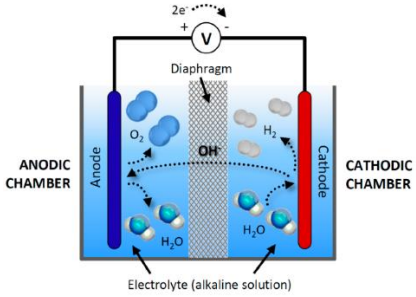

Fig. 3.3 General depiction of an alkaline electrolyser. Source: internet

PEM electrolysers use a solid polymer electrolyte known as Proton Exchange Membrane or Polymer Electrolyte Membrane. Due to recent advancements in technology, the cost of PEM has also come down to competitive levels with alkaline electrolysers. PEM technology has various advantages: it has a quick response ramp-up-and-down ability, and a vast dynamic operating range from 0 to 100% - meaning it is highly suitable for utilising additional renewable energy to generate hydrogen. They also have high current densities and high gas purity. But they too face a few problems like acidic corrosive environment, and high cost of components, and use of noble catalysts. Since this project aims to utilise the excess energy generated by solar panels to generate hydrogen, PEM has a clear advantage. [20]

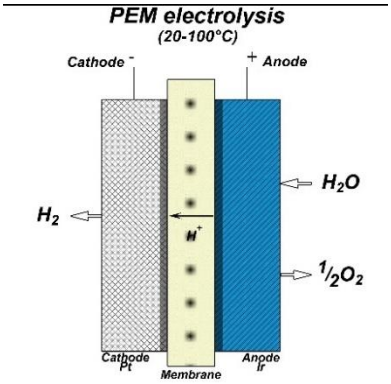

Fig. 3.4 General depiction of a PEM electrolyser. Source: internet

Solid Oxide Electrolysers use solid ceramic material as electrolyte. These electrolysers operate at a very high temperature, above 500^{o} C. Due to this, they can be far more efficient than the other two electrolysers. But due to their high operating temperatures, they cannot be used in this project as achieving those temperatures is not possible here. [20]

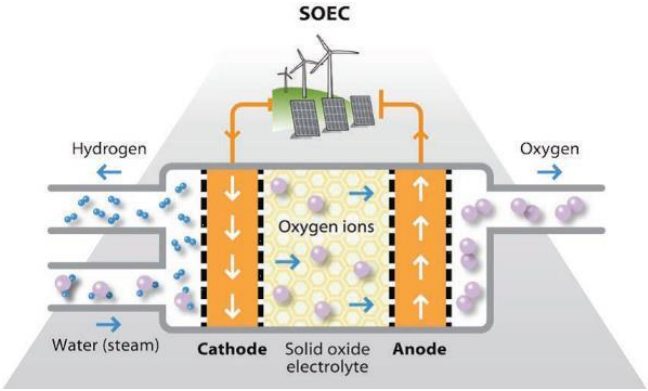

Fig. 3.5 General depiction of a solid oxide electrolyser. Source: internet

On the basis of the above discussion, PEM is chosen for this project to fulfil the role of electrolyser.

3.4 Fuel Cell Selection

A typical fuel cell generates electrical energy using hydrogen as a fuel by reacting with oxygen to produce water and heat. There are many types of fuel cells, based on electrolyte, fuel, and electrode material. They include Polymer Electrolyte Membrane Fuel Cell (PEMFC), alkaline, solid polymer, sulfuric and phosphoric acid, solid oxide, molten carbonate fuel cells.

Alkaline fuel cells can easily start from cold temperatures, and operate usually at 60-80 °C. Noble and active catalysts are needed due to the lower operating. But a major problem of alkaline cells is due to the interaction of CO_2 with the base electrolyte. CO_2 is in the flow of oxygen input as input of oxygen is generally from direct air. Hence it requires some scrubbing mechanism to remove the 0.04% CO_2 in inlet air. [21]

Sulfuric and phosphoric acid fuel cells are not so intolerant to CO_2, allowing the usage direct air and slightly impure hydrogen. But there exists the problem of corrosion which imposes restrictions on the materials for catalysts and electrodes. These operate at a temperature around 200° C that requires a platinum catalyst, which is susceptible to CO-poisoning at this temperature. Due to the indecent performance of the air electrode, the efficiencies of acid cells are lower compared to alkaline cells. [21]

In PEMFC, the electrolyte is a solid polymer layer which allows transmission of protons. Due to the limitations of membrane's thermal properties, PEMFCs operate at relatively lower temperature around 90 °C. They are also prone to contamination by CO, leading to a considerable reduction in efficiency. Additionally, cooling and output water management is essential for it to function appropriately. [21]

In solid polymer fuel cells, an example is using methanol directly as a fuel. It is still in development phase, with prototypes. Main problems include the lower electrochemical activity of CH_3OH in comparison to hydrogen, leading to lower cell efficiencies. Also, due to the miscibility of methanol in water, it might lead to crossing the water-saturated membrane causing corrosion and output gas challenges. [21]

The electrolyte of molten carbonate fuel cell is a molten mixture of K_2CO_3 and Li_2CO_3 which allows movement of CO_3^{2-} ions from cathode to anode. They operate at around 850 °C enabling the usage of nickel as catalyst. [21]

SOFCs are built wholly using solid-state materials with an electrolyte made of ion-conducting oxide ceramic. They operate at around 900-1000° C. They have many advantages over other fuel cell configurations: easier management of electrolyte, best efficiency among all the fuel cell technologies (50-60%), and internal reforming of hydrocarbon fuels can be done for CHP (Combined Heat & Power) uses. But they are very expensive to manufacture due to the requirement of costly high temperature alloys needed for the BOP structures. [21]

Based on the above discussion, PEM is chosen for this project to fulfil the role of fuel cell.

3.5 Thermally Insulated System Design

The main aim of the thermally insulated system is to utilise the maximum possible heat produced during the operation of electrolyser and fuel cell. Adding passive solar design would lead to greater thermal comfort and higher internal temperatures of the space. Hence, combining both passive solar building design and thermal insulation of the system would give the best possible results.

3.5.1 South-Facing Wall Design

The system being developed can be considered as a single room. Passive space heating systems can be divided into direct, indirect, and isolated gain systems.

In a direct gain system, the heated space is directly exposed to sunlight, which is converted to heat by absorbing surfaces. Greenhouses are direct gain systems. Fig 3.6 shows an example of a direct gain system. [18]

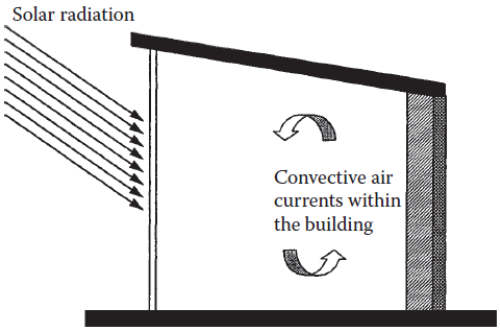

Fig. 3.6 Direct gain system [18]

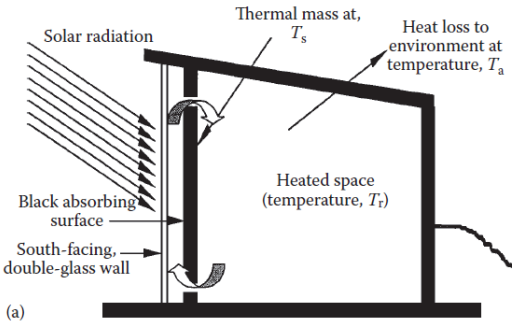

Fig. 3.7 Indirect gain system [18]

In an indirect gain system, a heat absorbing mass is present in between the internal space and the glass. This mass absorbs the irradiation from sun and retains it as heat. Examples include Trombe wall and solar wall. Fig 3.7 shows an example of an indirect gain system with a thermal storage wall.

The isolated gain is a modification of the indirect system with a definite thermal barrier between thermal storage and internal space by insulation or physical barrier. An example of this is a thermosyphon loop often used to heat domestic water. This loop is used to form a thermal storage wall or roof. [18]

Among the three systems, the indirect gain configuration is better for this project as it has a time lag in between solar radiation and heating of internal space, leading to better warmth during non-sunshine hours.

If the room is considered to be rectangular in floor/roof shape, then the longest wall should be the south facing wall. There are two types of walls in indirect gain systems namely Solar wall and Trombe wall.

A solar wall, in northern hemisphere, is a south-facing wall painted with black colour with a glazing on it. The black paint helps in absorbing the heat from sun's radiation and the glazing made of glass helps in insulating the wall from the external climate. This leads to storage of heat in the wall which slowly permeates inside the room. It causes delayed heating by storing energy in daytime and releasing it during the night with a lag. This helps in maintaining temperature of the room even during non-sunshine hours. [19]

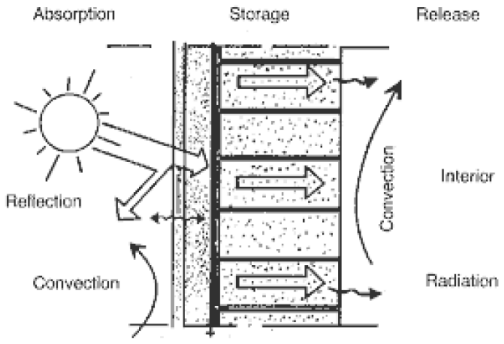

Fig. 3.8 Working of a solar wall [19]

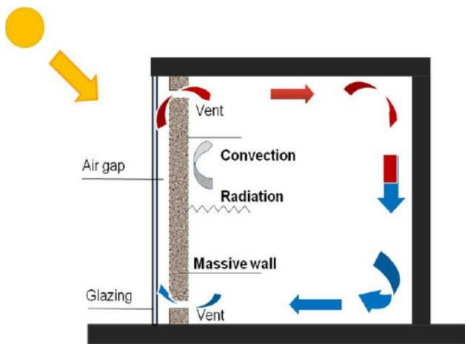

Fig. 3.9 Working of a Trombe wall. Source: internet

A Trombe wall is very similar to a solar wall, but with added ventilation. It has two vents, one at the top and the other at the bottom. The air trapped between the glass and the wall heats up and rises during the day. This leads to a convection current: cool air is drawn towards the lower opening and returned to the upper opening, increasing temperature significantly.

While the solar wall depends on the lag period in heat release for thermal comfort, the Trombe wall, on the other hand, has a lag in heat release and has a convective flow, which helps attain the temperature faster and provides more thermal comfort. A Trombe wall is found to have around 10% higher efficiency than a solar wall. [19]

The solar wall has almost zero maintenance; only the glass must be cleaned from the outside. Meanwhile, the Trombe wall has some basic maintenance as dust accumulates on the inner surface of glass due to convective flow, and shutters (ventilation openings) are to be closed at night.

Considering the above points, the Trombe wall is selected for the system design owing to its higher efficiency and more thermal comfort.

3.5.2 Components of Walls, Roof, and Floor

Different types of materials are used to cater to the needs of the functions of different components of the passive solar building. They are listed below.

Trombe Wall

Wooden plank between Trombe wall and ground, Wooden window frame, Mud/ Cement/ Concrete/ Water bottle bricks, Foam mattress between Trombe wall and side walls, Mortar, Plaster, Black paint on entire Trombe wall, Double Glass used as glazing

Other Walls

Punjabi Straw mixed with Ladakhi Clay to give lightweight insulating blocks, wood & wool waste from local Pashmina industry (all of them here are waste materials mostly)

Roof and Floor

Wooden floor, beams, planks, and shavings (all wooden)

Fig. 3.10 Components: Double glazing, straw, clay bricks, wooden shavings & plank. Source: internet

4. Modelling of Solar Hydrogen System

To analyse the performance of the system being developed, it is very important to have insights about how the system will behave under various operating conditions. Before directly developing a prototype, online modelling and simulation gives an idea of the possible scenarios and can help in understanding the limitations and problems in the system. For this project, modelling of solar PV, electrolyser, fuel cell, power electronics, hydrogen storage, and battery (if applicable) will be done. This report covers only the modelling of solar PV, electrolyser. The remaining components/subsystems will be modelled in the next stage.

4.1 Solar PV Modelling

Solar radiation is highly time dependent and varies from location to location. Hence, it is extremely important to capture the variability in the incoming solar energy over the 24 hours in a day and over the 12 months in a year. This will give a good idea of the minimum and maximum capacity of solar PV array, electrolyser, fuel cell, hydrogen storage and battery capacities.

Mathematical modelling of Solar PV can be done in two ways. The first method deals with currents and voltages and results in very detailed and exhaustive models. This makes it difficult to understand and increases the computational requirement and complexity of the model. But it also produces very accurate models in comparison to real life data. The second method deals with energy or power, making it much simpler and easier to understand. This reduces the computational requirement leading to lesser complex models. But they are less accurate than the models produced by the first method. This report presents three models for solar PV modelling, out of which two are based on the first method and one model is built on the second method.

4.1.1 Model 1

This model is based on the first method, adopted from [11]. A solar PV cell can be represented by electrical circuit in Fig. 4.1. Shunt resistance is neglected since it is very large.

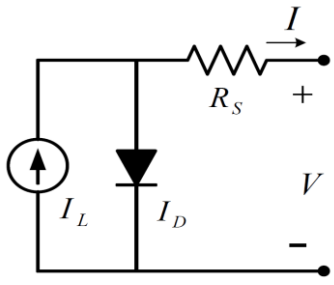

Fig. 4.1 Representative circuit diagram for a solar cell [11]

From the above circuit with a diode, current source and resistor, the load current can be calculated as follows:

$$I = I_L - I_D = I_L - I_o \left[\exp\left(\frac{V+IRs}{\alpha}\right) - 1\right] \quad (4.1)$$

Here, I represents the load current (A), I_L represents the light current or photocurrent (A), I_D represents the diode current (A), I_o represents the saturation current (A), V represents the output voltage (V), R_s represents the series resistance (Ω), α represents the thermal voltage timing completion factor (V). It can be noted that the light current is same as the short circuit current I_{SC} (A).

$$I_L = I_{SC} \tag{4.2}$$

This is a four-parameter model, where I_{SC}, I_o, R_s, and α need to be determined. I_L and I_{SC} are used interchangeably here. Light current can be given as

$$I_L = \frac{\phi}{\phi_{ref}}\left[I_{L,ref} + \mu_{I,SC}\left(T_C - T_{C,ref}\right)\right] \tag{4.3}$$

Here, φ represents the irradiance (W/m^2), φ_{ref} represents the reference irradiance (1000 W/m^2), $I_{L,ref}$ represents the photocurrent at 1000 W/m^2 and 25° C, $\mu_{I,sc}$ represents the temperature coefficient of I_{sc} (A/°C), Tc represents the solar cell temperature, $T_{c,ref}$ represents the reference temperature (25° C). The reference conditions (1000 W/m^2 and 25° C) are referred as Standard Test Conditions (STC)

Saturation current at any temperature can be expressed as a function of its reference value as

$$I_0 = I_{0,ref}\left(\frac{T_{C,ref}+273}{T_C+273}\right)^3 \exp\left[\frac{e_{gap}N_S}{q\alpha_{ref}}\left(1-\frac{T_{C,ref}+273}{T_C+273}\right)\right] \tag{4.4}$$

Here, $I_{o,ref}$ represents the saturation current at STC, e_{gap} represents the bandgap of the solar cell material (1.12 eV for Silicon), N_s represents the number of cells connected in series, q represents the charge of an electron (1.6*10^{-19} C), α_{ref} represents the value of α at STC.

$I_{o,ref}$ is given by

$$I_{0,ref} = I_{L,ref}\exp\left(-\frac{V_{oc,ref}}{\alpha_{ref}}\right) \tag{4.5}$$

Here, $V_{oc,ref}$ represents the open circuit voltage at STC.

α_{ref} is given by

$$\alpha_{ref} = \frac{2V_{mp,ref} - V_{oc,ref}}{\frac{I_{sc,ref}}{I_{sc,ref}-I_{mp,ref}} + \ln\left(1-\frac{I_{mp,ref}}{I_{sc,ref}}\right)} \tag{4.6}$$

Here, $V_{mp,ref}$ represents the voltage at maximum power point at STC, $I_{mp,ref}$ represents the current at maximum power point at STC, $I_{sc,ref}$ represents the short circuit current at STC.

α is related to temperature as follows

$$\alpha = \frac{T_C+273}{T_{C,ref}+273}\alpha_{ref} \tag{4.7}$$

Rs can be estimated by the following equation

$$R_S = \frac{\alpha_{ref} \ln\left(1 - \frac{I_{mp,ref}}{I_{SC,ref}}\right) + V_{OC,ref} - V_{mp,ref}}{I_{mp,ref}} \tag{4.8}$$

Voc can be calculated as

$$V_{oc} = \alpha \ln\left(\frac{I_{SC}+I_o}{I_o}\right) \tag{4.9}$$

Among all the above mentioned parameters, $I_{L,ref}$ (also referred as $I_{SC,ref}$), $V_{oc,ref}$, $I_{mp,ref}$, $V_{mp,ref}$, $\mu_{I,sc}$, N_s are provided by the manufacturer in the datasheet. These equations can be used to create a Simulink model to generate I-V characteristic curves for a solar module. This will be done in the next stage of the project in more detail.

4.1.2 Model 2

This model is based on the first method, adopted from [12]. The solar cell is represented by the following circuit with a single diode.

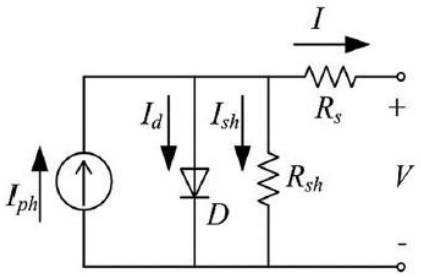

Fig. 4.2 Representative circuit diagram for a solar cell with shunt resistance [12]

From the above circuit with a diode, current source, shunt resistance and series resistance, the load current can be calculated as follows:

$$I = I_{\text{ph}} - I_0 \left\{ e^{\frac{q(V + R_s I)}{AKT}} - 1 \right\} - \frac{V + R_s I}{R_{\text{sh}}} \tag{4.10}$$

Here, I represents the load current, I_{ph} represents the photocurrent, I_o represents the saturation current, q represents the charge of an electron, V represents the output voltage, R_s represents the series resistance, A is the curve fitting factor, K is the Boltzmann constant, T is the cell temperature, R_{sh} represents the shunt resistance.

The typical value of A is taken to be 1.1 for Si solar cells [16] to account for the slight decrease in its value with increase in temperature.

Incorporating the number of cells in series, N_s and assuming shunt resistance to be infinite leads to the following equation

$$I = I_{\text{SC}} - I_o \left(e^{\frac{q(V + R_s I)}{N_s AKT}} - 1 \right) \tag{4.11}$$

Considering the open circuit condition of $I = 0$ gives

$$\frac{q}{N_s AKT} = \frac{\ln(\frac{I_{SC}}{I_0} + 1)}{V_{OC}} \tag{4.12}$$

Here, V_{oc} is the open circuit voltage.

Substituting (4.12) into (4.11) gives

$$I = I_{SC}\left[1 - \frac{I_o}{I_{SC}}\left(e^{\ln(\frac{I_{SC}}{I_0}+1)\frac{(V+R_s I)}{V_{OC}}} - 1\right)\right] \tag{4.13}$$

Let $k = I_{sc}/I_o$. Substituting the value of k in (4.13) gives

$$I = I_{SC}\left[1 - \frac{1}{k}(k+1)^{\frac{V+R_s I}{V_{OC}}} + \frac{1}{k}\right] \tag{4.14}$$

Generally, k has very large values because I_{sc} is much greater than I_o. This simplifies (4.14) into

$$I = I_{SC}\left(1 - k^{\frac{V+R_s I}{V_{OC}}-1}\right) \tag{4.15}$$

Considering currents and voltages at maximum power point under the reference conditions (STC) and rearranging (4.15) gives

$$k_{ref} = \sqrt[(\frac{V_{MPP,ref}+R_s I_{MPP,ref}}{V_{OC,ref}}-1)]{1 - \frac{I_{MPP,ref}}{I_{SC,ref}}} \tag{4.16}$$

With changes in temperature and irradiance, the short-circuit current and open-circuit voltage values of a solar module change. They are incorporated in the following equations

$$I_{SC} = I_{SC,ref}\left[1 + \alpha(T - T_{ref})\right]\frac{S}{S_{ref}} \tag{4.17}$$

$$V_{OC} = V_{OC,ref}\left[1 + a\ln\frac{S}{S_{ref}} + \beta(T - T_{ref})\right] \tag{4.18}$$

Here, T_{ref} represents the reference temperature (298 K), α represents the temperature coefficient of short-circuit current, S represents the solar irradiance, S_{ref} represents the STC solar irradiance (1000 W/m^2), a represents the irradiance correction factor of open-circuit voltage, β represents the temperature coefficient of open-circuit voltage. The typical value of a is taken to be 0.06 according to the standards of IEC 60891 (Photovoltaic devices - procedures for temperature and irradiance corrections to measured I-V characteristics)

The following translation equations are used

$$I = I_{ref}\frac{I_{SC}}{I_{SC,ref}} \tag{4.19}$$

$$V = V_{ref} + (V_{OC} - V_{OC,ref}) + R_s\,(I_{ref} - I) \tag{4.20}$$

With the help of STC conditions, R_s can be estimated as

$$R_s = \frac{V_{\mathrm{MPP,ref}} + \frac{I_{\mathrm{MPP,ref}}(V_{\mathrm{OC,ref}} - V_{\mathrm{MPP,ref}})}{(I_{\mathrm{SC,ref}} - I_{\mathrm{MPP,ref}})\ \ln(1 - \frac{I_{\mathrm{MPP,ref}}}{I_{\mathrm{SC,ref}}})}}{I_{\mathrm{MPP,ref}} + \frac{I^2_{\mathrm{MPP,ref}}}{(I_{\mathrm{SC,ref}} - I_{\mathrm{MPP,ref}})\ \ln(1 - \frac{I_{\mathrm{MPP,ref}}}{I_{\mathrm{SC,ref}}})}} \tag{4.21}$$

This method is robust and exhaustive, but there is a problem while developing the model. The value of k_{ref} can be derived from the reference conditions. But the value of k (required for obtaining the I-V curve mathematically) needs real life I-V data. Hence, this model cannot be used solely for modelling. It can be used in conjunction with some experimental data.

4.1.3 Model 3

This model is based on the first method, adopted from [13]. It accounts for maximum power only, generated by the solar module at a particular temperature and irradiance. Hence this model is given by a simple and single equation as follows

$$P_M = \frac{G}{G_o} P_{Mo} \left(1 + \gamma\ (T_c - T_o)\right) \tag{4.22}$$

Here, P_M represents the maximum power, G represents the solar irradiance, G_o represents the reference solar irradiance (1000 W/m^2), P_{Mo} represents the maximum power at STC, γ represents the temperature coefficient of maximum power, T_c represents the solar cell temperature, T_o represents the temperature at STC (25^o C).

The Simulink model of this equation is given below

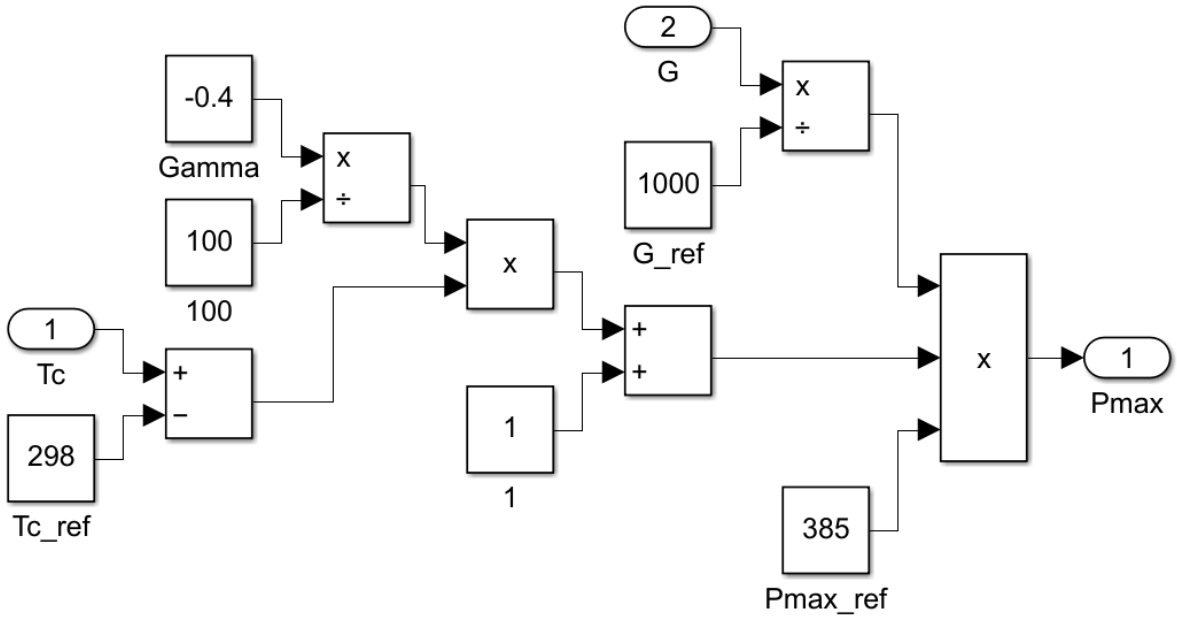

Fig 4.3 Simulink model of the solar cell based on power flow

Here, the inputs from the user are irradiance and temperature of the solar cell. The output is only maximum power at a particular temperature and irradiance. This model does not give the idea of the nature of currents and voltages. But it is useful when the system being developed needs to work based on power or energy flow. It makes the calculations and

modelling simpler. The parameters shown in the Simulink model belong to Polycab monocrystalline PERC 72 cell 5BB PV module. Technical specifications of the PV module at STC are given in Table 4.1.

Model	PIL 385HM
Maximum Power, Pmax (W)	385
Open Circuit Voltage, Voc (V)	48.72
Short Circuit Current, Isc (A)	10
Voltage at Maximum Power, Vmp (V)	40
Current at Maximum Power, Imp (A)	9.63
Module Efficiency (%)	19.37
Fill Factor (%)	79.06
Coefficient of Short Circuit Current (%/° C)	0.05
Coefficient of Open Circuit Voltage (%/° C)	-0.30
Coefficient of Maximum Power (%/° C)	-0.40

Table 4.1 Technical specifications of Polycab solar module. Source: internet

4.2 Electrolyser Modelling

The amount of hydrogen produced from electrolysis depends on multiple factors like electrolyser current, operating voltage, input power, electrode area, temperature, pressure. The excess renewable energy should be able to drive the electrolysis reaction. This can be ensured by using appropriate DC-DC converters (buck converters) to output a voltage sufficient to start electrolysis. Generally, the industrial electrolysers are operated in a range of voltage between 1.8 - 2.2 V. Hence, 2 V is considered to be the practical electrolyser voltage. Ideally, electrolyser should run at 1.23 V, but it cannot run at 1.23 V practically due to multiple losses. These include ohmic overpotential, concentration overpotential, and activation overpotential.

Mathematical modelling of an electrolyser has been done in many ways over the years. Parameters like partial pressure and molar flow rate of water, hydrogen, and oxygen, current density, active area, and the above listed overpotentials could be used to develop robust models that would represent a PEM electrolyser closely. This report deals with a simple electrolyser model, leaving scope for complex models in future work.

In the current electrolyser model, adopted from [14], the production rate of hydrogen is directly proportional to the electrolyser current. It is given by

$$N_{H2} = \frac{\eta_F N_C i_e}{2F} \tag{4.23}$$

Here, N_{H2} represents the number of moles of hydrogen produced per second (mol/s), η_F represents the Faraday efficiency, N_C represents the number of electrolyser cells in series, i_e represents the electrolyser current, F represents the Faraday constant.

Faraday efficiency is the ratio of maximum actual hydrogen produced in an electrolyser to the maximum theoretical hydrogen produced. It is given by

$$\eta_F = 96.5 \exp\left(\frac{0.09}{ie} - \frac{75.5}{ie^2}\right) \tag{4.24}$$

Equation (4.24) has been derived based on the empirical relation mentioned in [15] from the experimental data of HYSOLAR electrolyser of 10 kW, 5 bar. An assumption has been made during its derivation that the operating temperature of electrolyser is 40° C. In general, Faraday efficiency varies between 85 – 95%.

The developed Simulink model has been shown in Fig. 4.4. It takes electrolyser current as input and gives number of moles of hydrogen produced per second as output. N_C has been assigned an arbitrary value of 1.

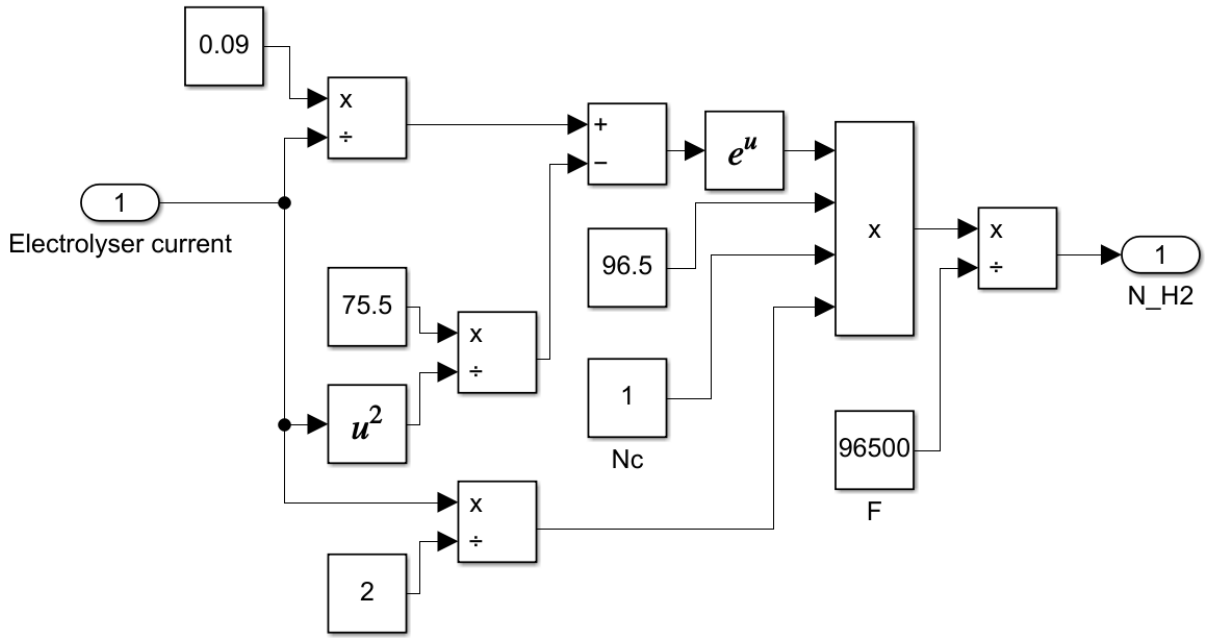

Fig. 4.4 Simulink model of electrolyser

4.3 Hydrogen Storage Modelling

The hydrogen produced by the electrolyser needs to be stored in a storage tank. Without a compressor or pump, hydrogen can fill up the tank/cylinder only until the pressure inside the tank reaches the electrolyser cathode pressure. This report considers a simple scenario of hydrogen storage without accounting for the compression requirements. The storage dynamics are given by the following equation, adopted from [17]

$$P_t - P_{ti} = z\left(\frac{N_{H2}\,R\,T_t}{M_{H2}V_t}\right) \tag{4.25}$$

Here, P_t represents the pressure of the tank (Pa), P_{ti} represents the initial pressure of the tank (Pa), z represents the compressibility factor which is a function of pressure, N_{H2} represents the number of moles of H_2 delivered to the tank per second (mol/s), R is the universal gas constant (J/mol-K), T_t represents the tank temperature (K), M_{H2} is the molar mass of hydrogen (kg/mol), V_t is the volume of the tank (m^3).

Compressibility factor varies with pressure and temperature. Upto 2000 psi (~138 bar), the compressibility factor is equal to 1 at room temperature. It becomes more than 1 at pressures greater than 2000 psi. Assuming that the tank pressure is less than 2000 psi in this case, compressibility factor is taken as 1. Tank volume is taken as 1 m^3, i.e., 1000 l. Initial tank

pressure value has been assumed to be 50 bar. Equation (4.25) is slightly re-arranged to obtain the tank pressure, P_t. The Simulink model of the hydrogen storage tank is shown in Fig. 4.5.

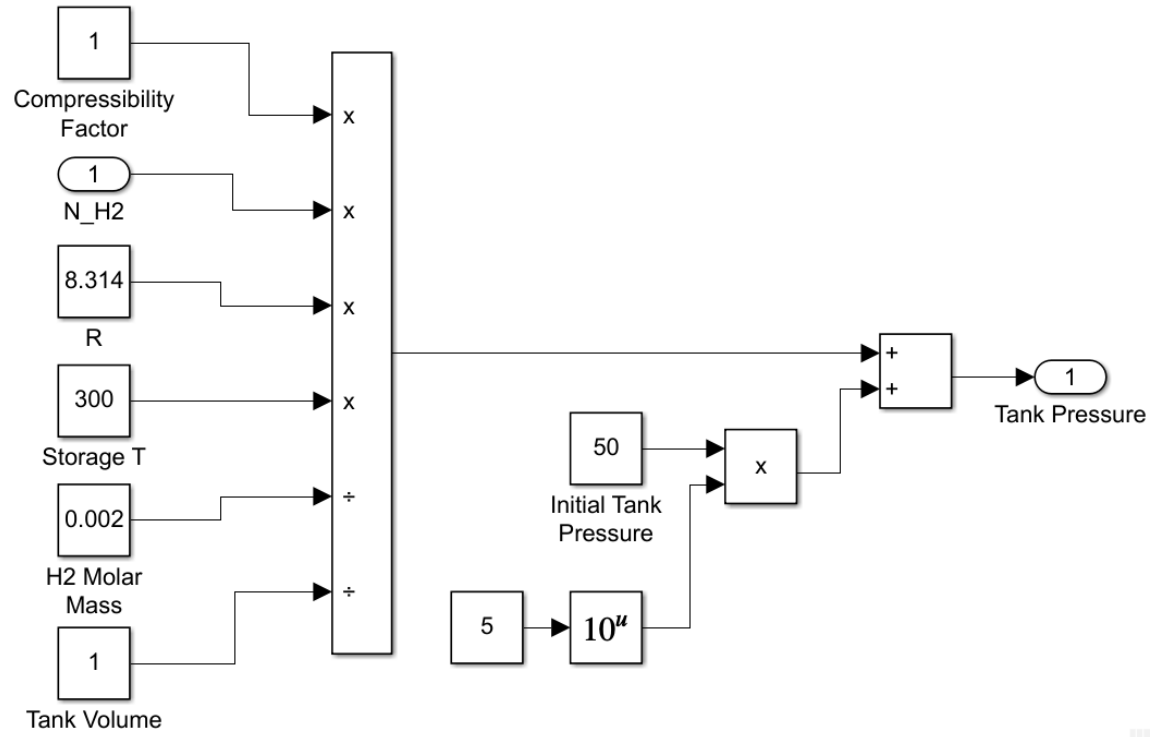

Fig. 4.5 Simulink model of hydrogen storage tank

4.4 Overall System Model

Integration of the solar PV subsystem, electrolyser subsystem, and hydrogen storage tank has been done which takes input of solar irradiance and solar cell temperature and gives output of tank pressure. A factor of 0.95 has been considered for the efficiency of power electronics which includes MPPT charge controller and DC-DC converter too. This gives the power input to electrolyser (equal to 0.95 times the power produced by solar modules). An electrolyser voltage of 2 V has been considered (the average operating voltage in industry). Hence, dividing the input power by 2 V gives the input electrolyser current. The number of moles of hydrogen produced per second helps in determining the tank pressure. The overall Simulink model is shown in Fig. 4.6.

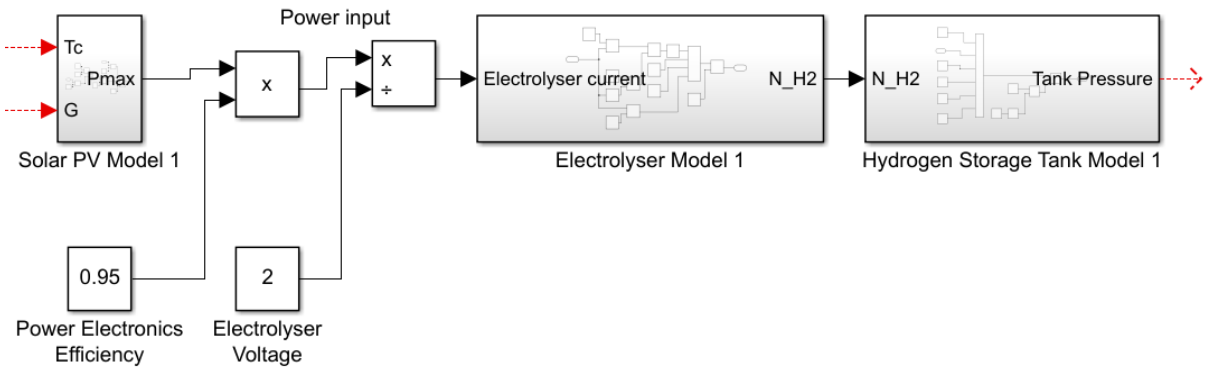

Fig. 4.6 Simulink model of entire solar hydrogen system

5. Conclusion

This project aims to build a multifunctional solar hydrogen system for the Indian Armed Forces. The round-trip efficiency of electricity to hydrogen to electricity via electrolyser-fuel cell path is generally around 35 %. But utilising the heat produced and not letting it get lost to the surroundings increases the effective efficiency to above 80-90 %. This makes the current solar hydrogen system viable.

With the help of this project, soldiers can get the following benefits:

i. **Electricity**: useful for electrolyser and general purposes
ii. **Hydrogen**: useful to generate electricity when the solar power supply is not possible. Also, exploring other benefits of hydrogen like hydrogen therapy and hydrogen fuel
iii. **Oxygen**: useful for medical purposes and health-related issues
iv. **Heat**: can warm themselves up when conditions outside are highly unfavourable or can comfort themselves for a brief period

This report gives an overview of various solar hydrogen production technologies. From this report, it can be concluded that non-integrated devices in photoelectrochemical water splitting devices are the best choice for the project. Monocrystalline Si PERC solar cells have been selected for the solar PV modules. Comparison of various electrolyser and fuel cell technologies led to the conclusion that PEM is the best option for both electrolyser and fuel cell. A detailed analysis of the thermally insulated system design was done with emphasis on the materials and configurations to be used.

Multiple models were considered for solar PV modelling and Simulink model was created for the lesser complex one. Relatively simpler models were adopted for the modelling of electrolyser and hydrogen storage tank. Simulink model was developed for only half of the entire solar hydrogen system. The remaining half including fuel cell and dynamic load behaviour is for future works.

6. Future Objectives

The scope of this project is huge. It includes developing robust and more exhaustive models for solar PV, electrolyser, fuel cell, hydrogen storage, thermal insulation, power electronics, and load. This will lead to a good Simulink model of the entire solar hydrogen system. Results of this model will help in determining the minimum and maximum capacities of all the technologies involved.

The possibility of the usage of a battery needs to be explored. The type of battery and the tank used for hydrogen storage needs to be reviewed. Power electronics like MPPT charge controller, DC-DC converters need to be finalised.

A CAD model of the entire system can help in visualisation to understand about the space utilisation and strategic placement of various equipment. Later, a small prototype of the solar hydrogen system can be constructed. After testing and analysing the prototype properly, a scaled-up version could be built, subject to approval.

References

[1] Privitera, S.M.S., M. Muller, W. Zwaygardt, M. Carmo, R.G. Milazzo, P. Zani, M. Leonardi, F. Maita, A. Canino, M. Foti, F. Bizzarri, C. Gerardi, and S.A. Lombardo. 2020. "Highly efficient solar hydrogen production through the use of bifacial photovoltaics and membrane electrolysis." *Journal of Power Sources* 473:228619.

[2] Lee, M., Turan B., Becker J.-P., Welter K., Klingebiel B., Neumann E., Sohn Y. J., Merdzhanova T., Kirchartz T., Finger F., Rau U., and Haas S. 2020. "A Bias-Free, Stand-Alone, and Scalable Photovoltaic–Electrochemical Device for Solar Hydrogen Production." *Advanced Sustainable Systems* 4:2000070.

[3] Kemppainen, Erno, Stefan Aschbrenner, Fuxi Bao, Aline Luxa, Christian Schary, Radu Bors, Stefan Janke, Iris Dorbandt, Bernd Stannowski, Rutger Schlatmann, and Sonya Calnan. 2020. "Effect of the ambient conditions on the operation of a large-area integrated photovoltaic-electrolyser." *Sustainable Energy Fuels* 4(9):4831-4847.

[4] Liu, Guanyu, Yuan Sheng, Joel W. Ager, Markus Kraft, and Rong Xu. 2019. "Research advances towards large-scale solar hydrogen production from water." *EnergyChem* 1(2):100014.

[5] Joshi, Anand S., Ibrahim Dincer, and Bale V. Reddy. 2011. "Solar hydrogen production: A comparative performance assessment." *International Journal of Hydrogen Energy* 36(17):11245-11257.

[6] Wang, Hongsheng, Hui Kong, Zhigang Pu, Yao Li, and Xuejiao Hu. 2020. "Feasibility of high efficient solar hydrogen generation system integrating photovoltaic cell/photon-enhanced thermionic emission and high-temperature electrolysis cell." *Energy Conversion and Management* 210:112699.

[7] Jonas, James. 2009. "THE HISTORY OF HYDROGEN." *AltEnergyMag*, April 1. Retrieved July 20, 2022 (https://www.altenergymag.com/article/2009/04/the-history-of-hydrogen/555/).

[8] Yilanci, A., I. Dincer, H.K. Ozturk. 2009. "A review on solar-hydrogen or fuel cell hybrid energy systems for stationary applications." *Progress in Energy and Combustion Science* 35(3):231-244.

[9] Shabani, Bahman., John Andrews. 2011. "An experimental investigation of a PEM fuel cell to supply both heat and power in a solar-hydrogen RAPS system." *International Journal of Hydrogen Energy* 36(9):5442-5452.

[10] Jafari, Moharrm., Davoud Armaghan, S.M. Seyed Mahmoudi, Ata Chitsaz. 2019. "Thermoeconomic analysis of a standalone solar hydrogen system with hybrid energy storage." *International Journal of Hydrogen Energy* 44(36):19614-19627.

[11] Krismadinata, Nasrudin Abd. Rahim, Hew Wooi Ping, Jeyraj Selvaraj. 2013. "Photovoltaic module modeling using simulink matlab." *Procedia Environmental Sciences* 17:537-546.

[12] Ding, K., X. Bian, H. Liu and T. Peng. 2012. "A MATLAB-Simulink-Based PV Module Model and Its Application Under Conditions of Nonuniform Irradiance." *IEEE Transactions on Energy Conversion* 27(4):864-872.

[13] Arab, A. Hadj., B. Taghezouit, K. Abdeladim, S. Semaoui, A. Razagui, A. Gherbi, S. Boulahchiche, I. Hadj Mahammed. 2020. "Maximum power output performance modeling of solar photovoltaic modules." *Energy Reports* 6(1):680-686.

[14] Ural, Zehra., Muhsin Tunay Gencoglu. 2014. “Design and simulation of a solar-hydrogen system for different situations.” *International Journal of Hydrogen Energy* 39(16):8833-8840.
[15] Ulleberg, O. 1998. *Stand-alone power systems for the future: optimal design, operation and control of solar-hydrogen systems*. Trondheim: Norwegian University of Science and Technology.
[16] Pindado, Santiago & Cubas, Javier & Manuel, Carlos. 2014. “Explicit Expressions for Solar Panel Equivalent Circuit Parameters Based on Analytical Formulation and the Lambert W-Function.” *Energies* 7:4098-4115.
[17] Görgün, Haluk. 2006. “Dynamic modelling of a proton exchange membrane (PEM) electrolyzer.” *International Journal of Hydrogen Energy* 31(1):29-38.
[18] Goswami, D. Yogi. 2015. *Principles of Solar Engineering.* 3rd ed. Boca Raton: CRC Press.
[19] Stauffer, V., D. Hooper. 2000. “Passive solar architecture in Ladakh.” *GERES.*
[20] Cockerill, Rob. “Electrolyser technologies PEM vs Alkaline electrolysis.” *Nel Hydrogen*, Retrieved October 10, 2022 (https://nelhydrogen.com/resources/electrolyser-technologies-pem-vs-alkaline-electrolysis/).
[21] University of Cambridge. “Types of Fuel Cells.” Retrieved October 11, 2022 (https://www.ceb.cam.ac.uk/research/groups/rg-eme/Edu/fuelcells/types-of-fuel-cells).